Overcoming Morphological and Efficiency Limit in All-Polymer Solar Cells by Designing Conjugated Random Copolymers Containing Naphtho[1,2-c:5,6-c']bis([1,2,5]thiadiazole)] Moiety

*Ruihao Xie[†a], Zhenye Li[†a], Wenkai Zhong[†a], Lei Ying[*a], Qin Hu[c,d], Feng Liu[*b], Ning Li[e], Thomas P. Russell[c,d], Fei Huang[*a], and Yong Cao[a]*

[a] Institute of Polymer Optoelectronic Materials and Devices, State Key Laboratory of Luminescent Materials and Devices, South China University of Technology, Guangzhou 510640, China

[b] Department of Physics and Astronomy, and Collaborative Innovation Center of IFSA (CICIFSA), Shanghai Jiao Tong University, Shanghai 200240, China

[c] Materials Sciences Division, Lawrence Berkeley National Laboratory, Berkeley, CA 94720, USA

[d] Department of Polymer Science and Engineering, University of Massachusetts Amherst, 120 Governors Drive, Amherst, MA 01003, USA

[e] Institute of Materials for Electronics and Energy Technology (i-MEET), FAU Erlangen-Nürnberg, 91058 Erlangen, Germany

1. Synthesis

The monomers of 5,10-bis(5-bromo-4-(2-octyldodecyl)thiophen-2-yl)naphtho[1,2-*c*:5,6-*c*']bis([1,2,5]thiadiazole) (NT-Br$_2$) were synthesized according to the previous procedures.[1] 2,5-Bis(trimethylstannyl)thiophene (Th-Sn$_2$) and 2,6-dibromo-4,8-bis (5-(2-ethylhexyl)thiophen-2-yl)benzo[1,2-*b*:4,5-*b*']dithiophene (BDT-Br$_2$) were purchased from SunaTech Inc. The polymer N2200 was synthesized by Stille coupling, similarly as previously reported.[2]
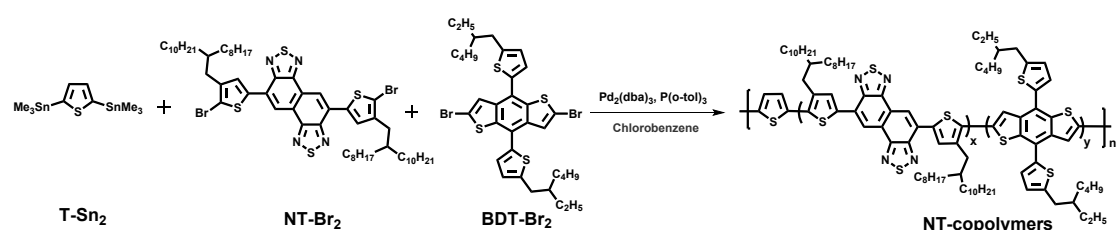
Scheme S1. Chemical structures and synthesis of the polymers.

Synthesis of NT00. The compounds of Th-Sn$_2$ (82.0 mg, 0.2 mmol), BDT-Br$_2$ (147.3 mg, 0.2 mmol), tris(dibenzylideneacetone)dipalladium(0) (Pd$_2$(dba)$_3$) (1.8 mg) and tri(o-tolyl) phosphine (P(o-tol)$_3$) (4.8 mg) were dissolved in anhydrous chlorobenzene (3 mL) under a nitrogen atmosphere. The reaction mixture was heated at 140 °C with vigorous stirring for 48 h. Then, the bromo-terminal groups were capped with 2-(tributylstannyl)thiophene (0.1 mL), refluxing for 2 h. After that, the trimethylstannyl-terminal groups were capped with 2-bromothiophene (0.2 mL), refluxing for another 2 h. After cooling to room temperature, the polymer was precipitated from the solution into methanol and was collected by filtration and then successively purified by Soxhlet extraction with methanol (12 h), hexane (12 h) and chloroform (12 h). The chloroform fraction was collected by precipitated from methanol again. The resulting polymer was then dried under vacuum for 1 day to get the polymer **NT00**. Yield: 107.0 mg (81 %).

Synthesis of NT10. The compounds of Th-Sn$_2$ (41.0 mg, 0.1 mmol), BDT (66.3 mg, 0.09 mmol), NT-Br$_2$ （11.3 mg, 0.01mmol）, Pd$_2$(dba)$_3$ (1.8 mg) and P(o-tol)$_3$ (4.8 mg) were dissolved in anhydrous chlorobenzene (1.5 mL) under a nitrogen atmosphere. The reaction mixture was heated at 140 °C with vigorous stirring for 48 h. Then, the bromo-terminal groups were capped with 2-(tributylstannyl)thiophene (0.1 mL), refluxing for 2 h. After that, the trimethylstannyl-terminal groups were capped

with 2-bromothiophene (0.2 mL), refluxing for another 2 h. After cooling to room temperature, the polymer was precipitated from the solution into methanol and was collected by filtration and then successively purified by Soxhlet extraction with methanol (12 h), hexane (12 h), dichloromethane (12 h) and chloroform (12 h). The chloroform fraction was collected by precipitated from methanol again. The resulting polymer was then dried under vacuum for 1 day to get the polymer **NT10**. Yield: 63.0 mg (90 %).

Synthesis of NT20.

According to the polymerization method above, the monomers of Th-Sn$_2$ (41.0 mg, 0.1 mmol), BDT-Br$_2$ (58.9 mg, 0.08 mmol), NT-Br$_2$ （22.5 mg, 0.02mmol） were used. The polymer **NT20** was obtained successfully. Yield: 65.0 mg (88 %).

Synthesis of NT30.

According to the polymerization method above, the monomers of Th-Sn$_2$ (41.0 mg, 0.1 mmol), BDT-Br$_2$ (51.6 mg, 0.07 mmol), NT-Br$_2$ （33.8 mg, 0.03mmol） were used. The polymer **NT30** was obtained successfully. Yield: 69.3 mg (89 %).

Synthesis of NT40.

According to the polymerization method above, the monomers of Th-Sn$_2$ (41.0 mg, 0.1 mmol), BDT-Br$_2$ (44.2 mg, 0.06 mmol), NT-Br$_2$ （45.1 mg, 0.04 mmol） were used. The polymer **NT40** was obtained successfully. Yield: 65.3 mg (80 %).

Synthesis of NT50.

According to the polymerization method above, the monomers of Th-Sn$_2$ (41.0 mg, 0.1 mmol), BDT-Br$_2$ (36.8 mg, 0.05 mmol), NT-Br$_2$ （56.4 mg, 0.05mmol） were used. The polymer **NT50** was obtained successfully. Yield: 70.2 mg (82 %).

Synthesis of NT60.

According to the polymerization method above, the monomers of Th-Sn$_2$ (41.0 mg, 0.1 mmol), BDT-Br$_2$ (29.5 mg, 0.04 mmol), NT-Br$_2$ （67.6 mg, 0.06mmol） were used. The polymer **NT60** was obtained successfully. Yield: 76.4 mg (85 %).

Synthesis of NT70.

According to the polymerization method above, the monomers of Th-Sn$_2$ (41.0 mg, 0.1 mmol), BDT-Br$_2$ (22.1 mg, 0.03 mmol), NT-Br$_2$ （78.9 mg, 0.07mmol） were used. The polymer **NT70** was obtained successfully. Yield: 83.2 mg (89 %).

Synthesis of NT80.

According to the polymerization method above, the monomers of Th-Sn$_2$ (41.0 mg,

0.1 mmol), BDT-Br$_2$ (14.7 mg, 0.02 mmol), NT-Br$_2$ （90.2 mg, 0.08 mmol） were used. The polymer **NT80** was obtained successfully. Yield: 81.2 mg (83 %).

Synthesis of NT90.

According to the polymerization method above, the monomers of Th-Sn$_2$ (41.0 mg, 0.1 mmol), BDT-Br$_2$ (7.4 mg, 0.01 mmol), NT-Br$_2$ （101.5 mg, 0.09mmol） were used. The polymer **NT90** was obtained successfully. Yield: 82.0 mg (81 %).

Synthesis of NT100. The synthesis procedures of **NT100** were described in our previous paper. Yield: 96.8 mg (92 %).


2. Measurements and Characterization

The number-average molecular weight (M_n) and polydispersity index (PDI) of copolymers were determined on a Polymer Laboratories PL-GPC 220 using 1,2,4-trichlorobenzene as the eluent at 150 °C vs. polystyrene standards (Table S1). The absorption spectra of the samples as films and as a solution were obtained using a UV-Vis spectrometer (HP 8453, photodiode array type) in the wavelength range 300 to 1000 nm. Photoluminescence (PL) spectra were recorded on a Jobin-Yvon FluoroMax-4 spectrofluorometer. The electrochemical cyclic voltammetry experiments were conducted on a CHI600D electrochemical workstation with a platinum working electrode and a Pt wire counter electrode at a scanning rate of 50 mV s^{-1} against an Ag/Ag$^+$ (0.1 M of AgNO$_3$ in acetonitrile) reference electrode with a nitrogen-saturated anhydrous solution of 0.1 mol L^{-1} tetrabutylammonium hexafluorophosphate in acetonitrile. Tapping-mode AFM images were obtained using a Bruker Multimode 8 Microscope. Transmission electron microscopy images were obtained using a JEM 2100F microscope. Grazing incidence X-ray diffraction characterization of the thin films was performed at the Advanced Light Source on beamline 7.3.3, Lawrence Berkeley National Lab (LBNL). Thin film samples were prepared on wafer substrates. The scattering signal was recorded on a 2D detector (Pilatus 2M) with a pixel size of 0.172 mm by 0.172 mm. The samples were ≈15 mm long in the direction of the beam path, and the detector was located at a distance of ≈300 mm from the sample center (distance calibrated using a silver behenate standard). The incidence angle of 0.16° was chosen which gave the optimized signal-to-background ratio. The beam energy was 10 keV, operating at top-off mode. Typically, 10 seconds exposure time was used to collect diffraction signals. All GIXD

experiments were done in helium atmosphere. The data was processed and analyzed using Nika software package. Resonant soft X-ray scattering was performed at beamline 11.0.1.2 Advanced Light Source, LBNL. Thin film samples were spin-casted on top of the PEDOT:PSS covered Si wafers under exactly the same condition as those for the fabrication of solar cell devices. Then BHJ thin films were floated and transferred onto silicon nitride membrane windows. The scattering was done in transmission mode and signals were collected in vacuum using Princeton Instrument PI-MTE CCD camera.

3. Optical and Electrochemical Properties

Here we used the potential ferrocene/ferrocenium (Fc/Fc$^+$) redox couple as the standard. Under the current measurement conditions, the potential of Fc/Fc$^+$ couple was measured as 0.30 V regarding to the reference electrode. Assuming that the Fc/Fc$^+$ redox couple has an absolute potential of –4.80 V to vacuum, the highest occupied molecular orbital energy levels (E_{HOMO}) is calculated as $E_{HOMO} = -e\ (E_{ox} + 4.80 - 0.30)$ (eV), and the lowest unoccupied molecular orbital energy levels (E_{LUMO}) is calculated as $E_{LUMO} = -e\ (E_{red} + 4.80 - 0.30)$ (eV). The CV characteristics of NT-copolymers as shown in Fig. S1 and the corresponding electrochemical data were summarized in Table S1.
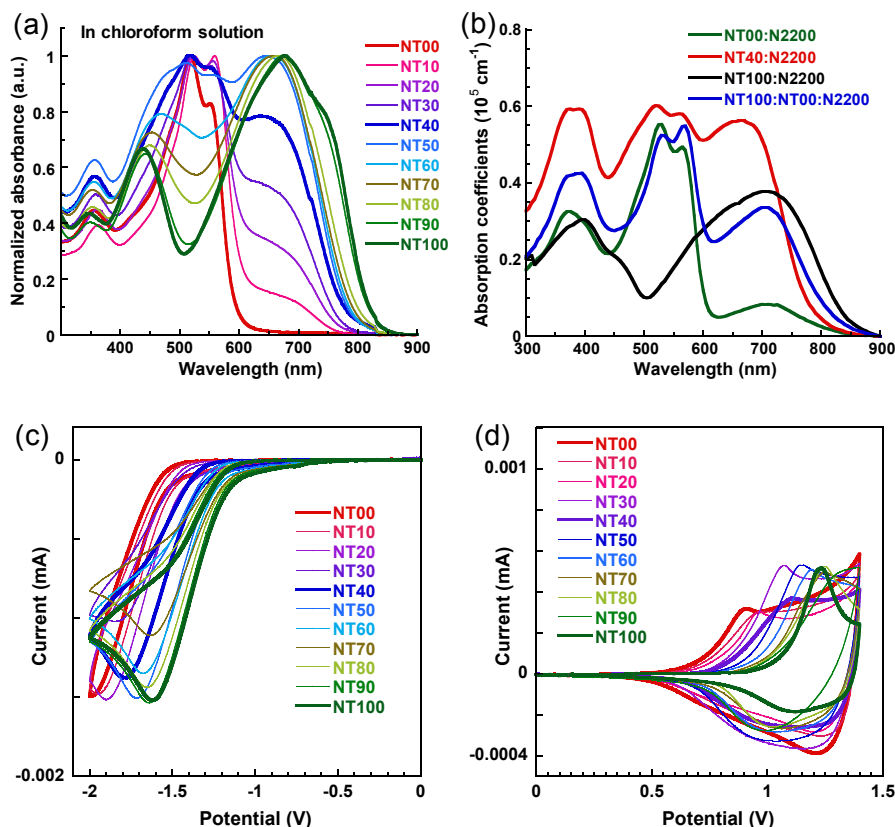
Fig. S1 Normalized UV absorption spectra of NT-copolymers in chloroform solution (a); UV-vis absorption spectra of the blend films based on NT-copolymers and N2200 (b); cyclic voltammograms of the polymers, electrochemical reduction (c); electrochemical oxidation (d).

Table S1. Molecular weight, optical and electrochemical properties of polymers

Polymer	M_n (kDa)	PDI	λ_{onset} (nm)	E_g^{opt} (eV)	E_{ox} (V)	E_{red} (V)	E_{HOMO} (eV)	E_{LUMO} (eV)
NT00	47.5	2.06	627	1.98	0.71	-1.55	-5.21	-2.95
NT10	57.7	2.40	753	1.65	0.72	-1.50	-5.22	-3.00
NT20	59.9	2.16	762	1.63	0.74	-1.42	-5.24	-3.08
NT30	58.5	2.29	782	1.59	0.82	-1.37	-5.32	-3.13
NT40	61.6	2.36	787	1.58	0.84	-1.28	-5.34	-3.22
NT50	53.4	2.11	791	1.57	0.92	-1.24	-5.42	-3.26
NT60	55.2	2.03	793	1.56	0.95	-1.20	-5.45	-3.30
NT70	50.4	2.11	798	1.55	0.97	-1.15	-5.47	-3.35
NT80	60.8	2.08	804	1.54	0.99	-1.12	-5.49	-3.38
NT90	63.2	1.99	813	1.53	1.00	-1.10	-5.50	-3.40
NT100	79.9	2.01	830	1.49	1.02	-1.10	-5.52	-3.40

4. Photovoltaic Properties

Fabrication of Polymer Solar Cells: The indium tin oxide (ITO) coated glass substrates were cleaned by sonication in detergent, deionized water, acetone, and isopropyl alcohol. They were dried in an oven at 75 °C for 12 h before use. After exposure to oxygen plasma for 2 min, PEDOT:PSS (*CLEVIOS* P VP Al 4083) was spun onto the substrates at 3000 rpm for 30 s. The coated substrates were annealed at 150 °C on a hot plate in air for 15 min to produce 40-nm thin films. After annealing, they were transferred to a glove box under an N_2 atmosphere. The blended films were obtained by spin-coating a chloroform (CF) solution containing DIO (0.5 vol %). The photoactive layers were thermally annealed at 120 °C for 10 min, and 5-nm PFN-Br was spin-coated as the cathode interface. The film thickness was maintained at 100 ± 10 nm. A 100-nm argentum (Ag) layer was then thermally deposited onto the active layer through a shadow mask in a vacuum chamber with a base pressure of 2×10^{-6} mbar. The effective area of the devices (0.04 cm^2) was determined by the shadow mask. The current density-voltage (*J-V*) characteristics were measured under a computer controlled Keithley 2400 sourcemeter under 1 sun, AM 1.5 G solar simulator (Taiwan, Enlitech SS-F5). The EQE spectra were measured on a commercial EQE system (Taiwan, Enlitech, QE-R3011).
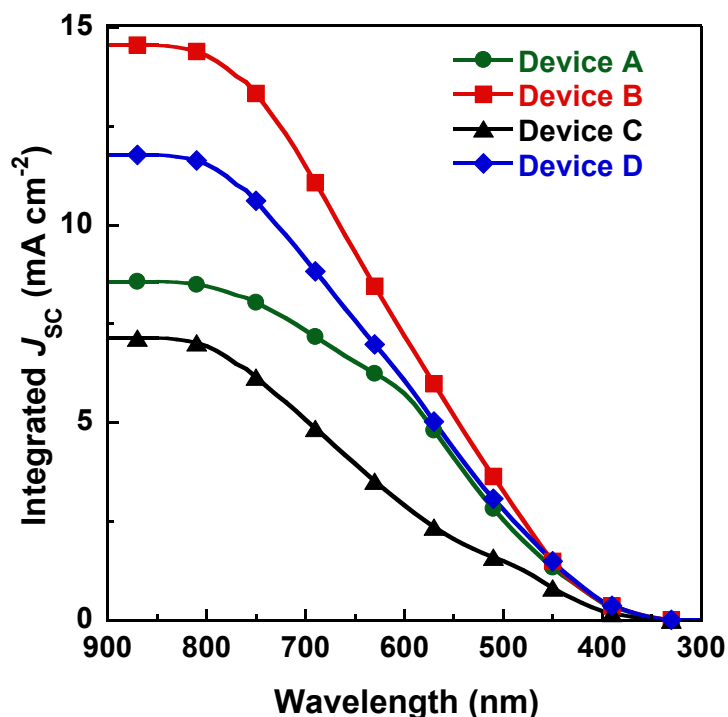
**Fig. S2** Integrated J_{SC} values calculated from EQE spectrum.
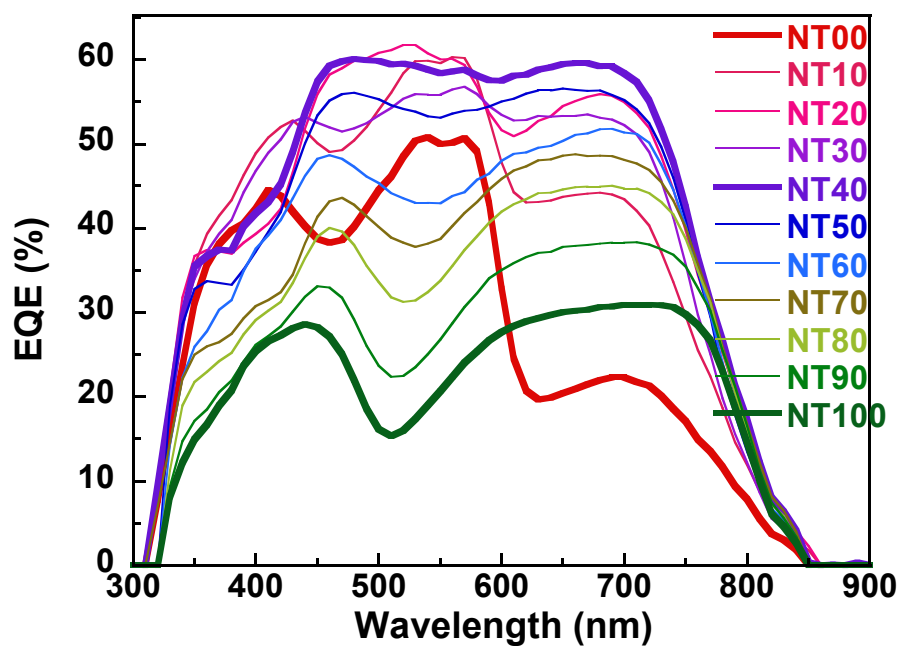
Fig. S3 EQE spectra of binary all-PSCs devices measured under AM 1.5G at 100 mW cm^{-2} illumination.

Table S2. Photovoltaic parameters of binary all-PSCs measured under AM1.5 Illumination at 100 mW/cm^2.

D:A (2:1)[a]	V_{OC} (V)	J_{SC} (mA cm^{-2})	FF (%)	PCE (%)
NT00:N2200	0.68	8.49	54.03	3.20
NT10:N2200	0.73	13.30	57.58	5.61
NT20:N2200	0.75	14.94	59.95	6.71
NT30:N2200	0.77	14.29	63.33	7.02
NT40:N2200	0.80	14.87	67.41	8.06
NT50:N2200	0.80	14.60	66.27	7.70
NT60:N2200	0.80	12.23	58.53	5.62
NT70:N2200	0.81	11.02	57.86	5.17
NT80:N2200	0.81	11.00	56.85	5.07
NT90:N2200	0.82	9.07	56.91	4.24
NT100:N2200	0.83	7.43	56.50	3.51

[a] All of the blend films are processed by CF with 0.5vol%DIO and treated with 120 ºC for 10 min.
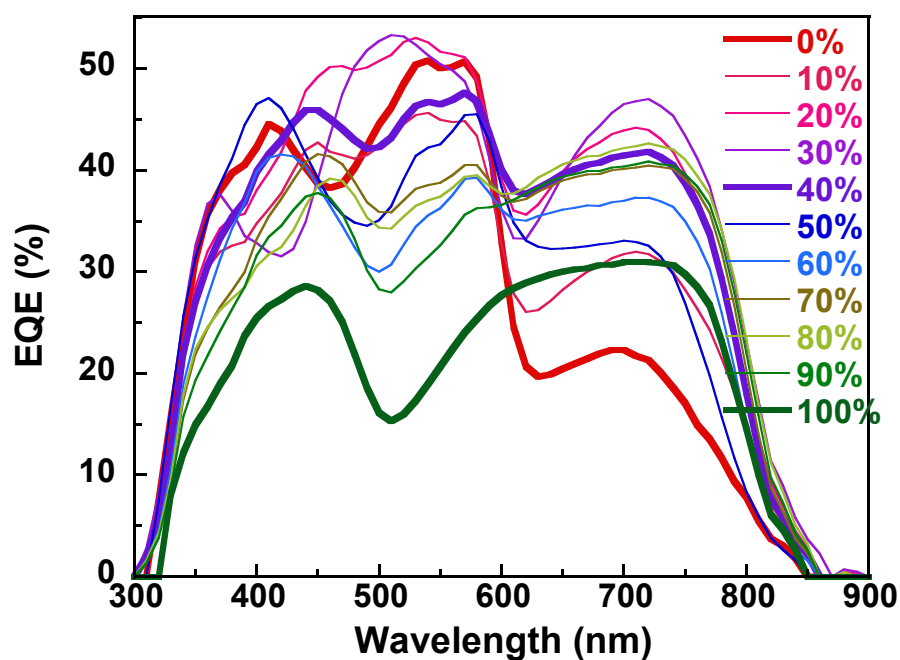
Fig. S4 EQE spectra of all-PSCs devices composed of NT00:NT100:N2200 with various weigh ratio of NT100 (0% to 100% in 10% increments).

Table S3. Photovoltaic parameters of ternary all-PSCs measured under AM1.5 Illumination at 100 mW cm^{-2}

NT00:NT100:N2200[a]	V_{OC} (V)	J_{SC} (mA cm^{-2})	FF (%)	PCE (%)
1.8:0.2:1 (10%)	0.73	8.49	56.97	3.54
1.6:0.4:1 (20%)	0.66	12.13	46.12	3.69
1.4:0.6:1 (30%)	0.63	10.71	48.90	3.29
1.2:0.8:1 (40%)	0.67	12.28	58.97	4.81
1:1:1 (50%)	0.71	11.85	53.97	4.54
0.8:1.2:1 (60%)	0.66	10.88	57.96	4.15
0.6:1.4:1 (70%)	0.64	10.33	60.54	4.02
0.4:1.6:1 (80%)	0.60	10.41	54.84	3.43
0.2:1.8:1 (90%)	0.64	10.17	55.25	3.57

[a] All of the blend films are processed by CF with 0.5vol%DIO and treated with 120 ^{o}C for 10 min.
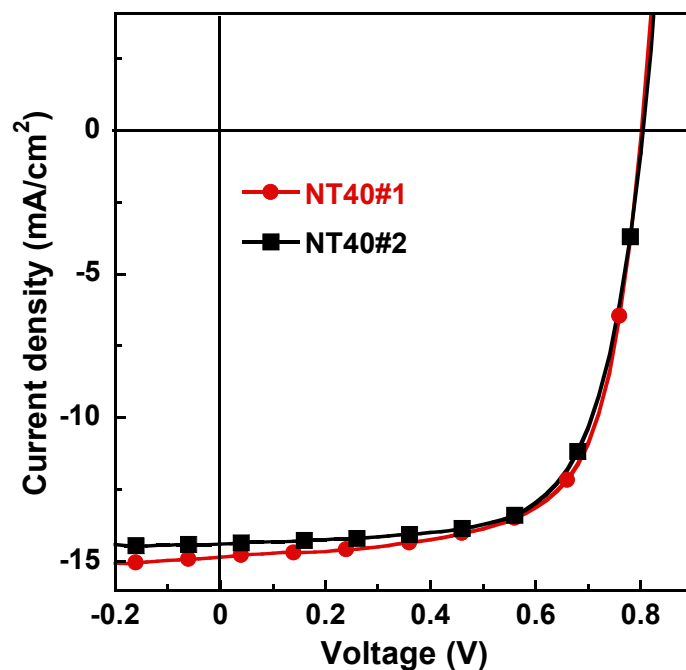
Fig. S5 *J-V* characteristics of NT40:N2200 devices with different polymer batches measured under AM 1.5G at 100 mW cm^{-2} illumination

**Table S4.** Solar cell characteristics of NT40:N2200 devices with different polymer batches

Polymer[a]	M_n (kDa)	*PDI*	V_{OC} (V)	J_{SC} (mA cm^{-2})	FF (%)	PCE$_{avg}$[d] (%)
NT40#1	61.6	2.36	0.80	14.87	67.41	7.92
NT40#2	59.9	2.18	0.80	14.39	67.95	7.87

[a] All of the blend films are processed by CF with 0.5 vol % DIO and treated with 120 °C for 10 min; Device structure: ITO/PEDOT:PSS/active layer/PFN-Br/Ag.

5. Charge Generation Properties

Photoluminescence (PL) measurements were conducted to investigate the exciton dissociation and charge transfer behavior, with the relevant characteristics shown in Fig. S6. To further investigate the exciton dissociation and carrier generation, we measured the dependence of the photocurrent density (J_{ph}) on the effective voltage (V_{eff}) under illumination at 100 mW cm^{-2} on a double-logarithmic scale (Fig. S7). The photocurrent density (J_{ph}) is defined as $J_{ph} = J_L - J_D$, where J_L and J_D represent the current densities measured under illumination and in the dark, respectively. The effective voltage (V_{eff}) is defined as $V_{eff} = V_{bi} - V_{appl}$, where V_{bi} is the voltage when $J = 0$ (the built-in voltage), and V_{appl} is the applied voltage. The relevant parameters obtained from J_{ph}–V_{eff} curves were showed in Table S5.
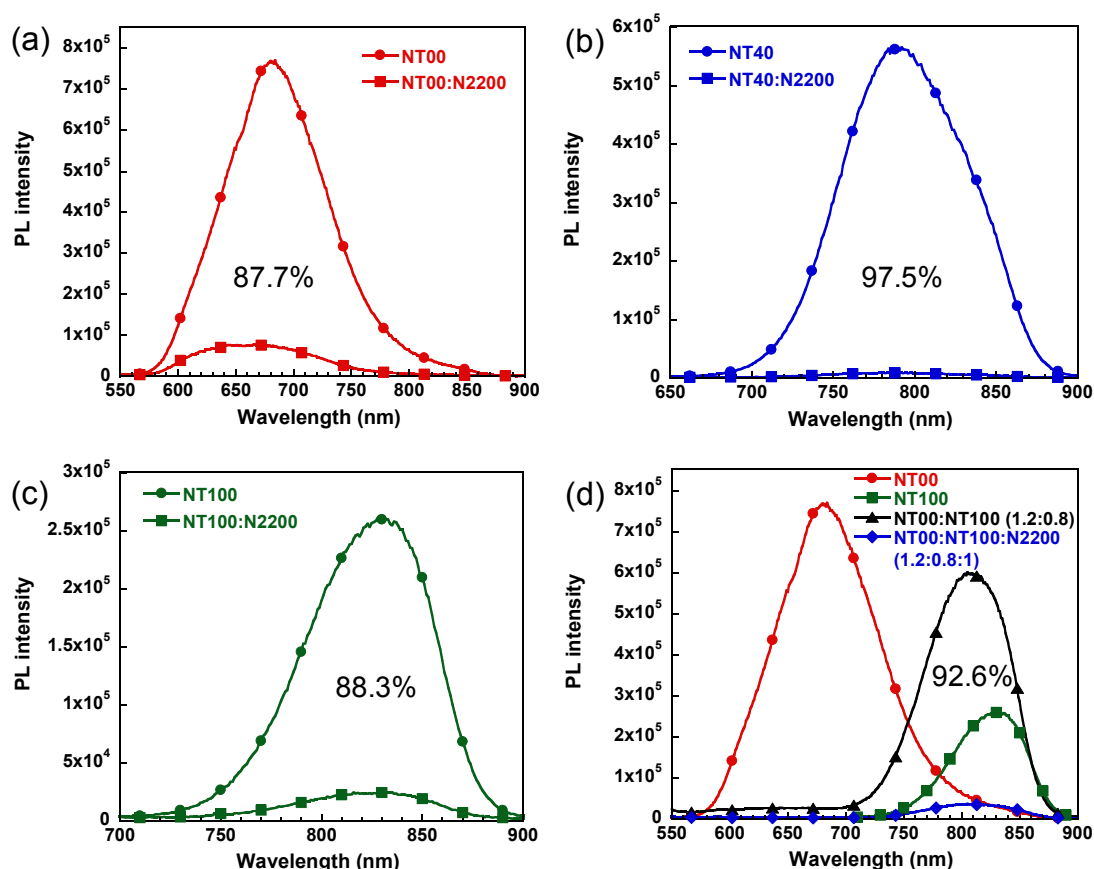
**Fig. S6** PL spectra of the pure polymer films and their corresponding blend films, excited at 500 nm.

Table S5. Relevant parameters obtained from J_{ph}–V_{eff} curves

Device[a]	J_{ph} (mA cm^{-2})	J_{sat} (mA cm^{-2})	G_{max} (m^{-3} s^{-1})	$P (E, T)$[b]	L (nm)
A	7.60	8.41	5.62×10^{27}	0.904	~100
B	14.54	15.48	1.03×10^{28}	0.939	~100
C	6.97	8.84	5.91×10^{27}	0.788	~100
D	11.95	13.07	8.73×10^{27}	0.914	~100

[a] All of the blend films are processed by CF with 0.5vol%DIO and treated with 120 °C for 10 min. The weight ratio of photoactive layer for device A: NT00:N2200 (2:1, wt:wt), device B: NT40:N2200 (2:1, wt:wt), device C: NT100:N2200 (2:1, wt:wt) and device D: NT00:NT100:N2200 (1.2:0.8:1, wt:wt:wt).

6. Space Charge Limited Current (SCLC) mobilities

The hole mobility was measured in a hole-only device composed of ITO/PEDOT:PSS/active layer/Ag. The electron mobility was measured in an electron-only device composed of ITO/ZnO/active layer/PFN-Br/Al. The mobility μ was determined by fitting the dark current to the model of a single carrier SCLC, which is described by Equation: $J = (9/8)\varepsilon_0\varepsilon_r\mu V^2/d^3$, where J is the current density, μ is the charge (hole or electron) mobility at zero field, ε_0 is the free-space permittivity, ε_r is the relative permittivity of the material, d is the thickness of the active layer, and V is the effective voltage $V-V_{bi}$. From the plots of $J^{1/2}$ versus V as shown in Fig. S7, the calculated hole-mobility (μ_h) and electron-mobility (μ_e) values are summarized in Table S6.
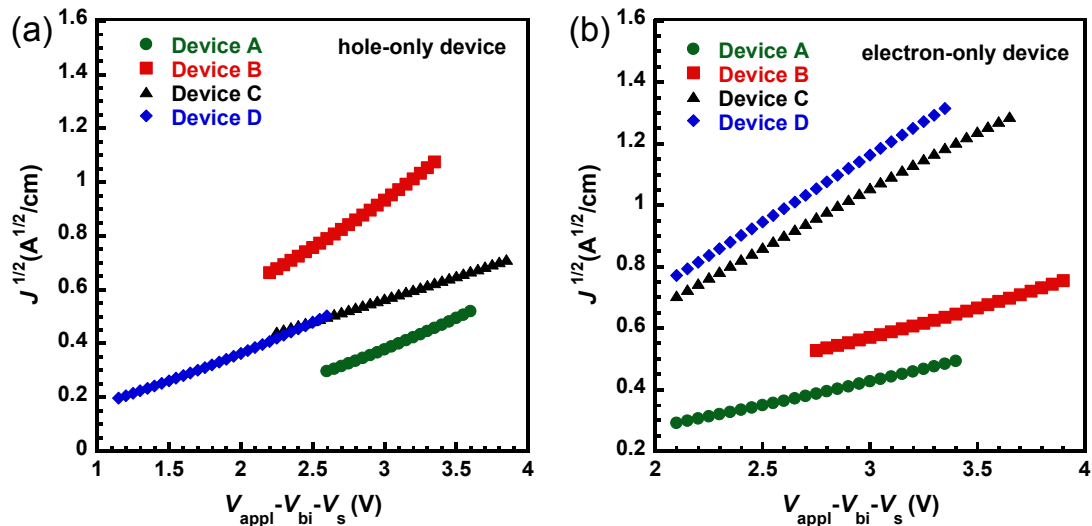
Fig. S7 $J^{1/2}$–V characteristics of devices based on NT00:N2200 (2:1, wt:wt, device A), NT40:N2200 (2:1, wt:wt, device B), NT100:N2200 (2:1, wt:wt, device C) and NT00:NT100:N2200 (1.2:0.8:1, wt:wt:wt, device D).

7. Charge Recombination Properties

To get insight into the recombination mechanisms of all-PSCs devices, the J_{SC} and V_{OC} versus light intensity (P_{light}) characteristics for devices were measured to reveal the charge recombination dynamics in the photoactive layer. The power law dependence of J_{SC} on the illumination intensity can generally be expressed as $J_{SC} \propto (P_{light})^S$ in organic solar cells, where P_{light} is the light intensity and S is the exponential factor, which is close to unity when the bimolecular recombination is weak in the device. By studying V_{OC} as a function of P_{light}, we can extract the slope of nkT/q in the plot of V_{OC} versus the natural logarithm of P_{light}, where n equals to one implies predominate bimolecular recombination and an enhanced dependence of V_{OC} on P_{light} ($2kT/q$) is a signature of trap-assisted monomolecular recombination. The relevant characteristics and parameters are summarized in Table S6.

Table S6. Relevant parameters obtained from J_{ph}–V_{eff} curves.

| Device[a]	n (V_{OC}-P_{light})	S (J_{SC}-P_{light})	μ_h (cm^{2}V^{-1}s^{-1})	μ_e (cm^{2}V^{-1}s^{-1})	μ_h/μ_e
A	1.42	1.032	2.10×10^{-4}	1.02×10^{-4}	2.06
B	1.20	1.033	6.67×10^{-4}	2.31×10^{-4}	2.89
C	2.13	1.035	8.28×10^{-5}	4.26×10^{-4}	0.19
D	1.59	1.026	9.08×10^{-5}	3.90×10^{-4}	0.23

[a] All of the blend films are processed by CF with 0.5vol%DIO and treated with 120 °C for 10 min. The weight ratio of photoactive layer for device A: NT00:N2200 (2:1, wt:wt), device B: NT40:N2200 (2:1, wt:wt), device C: NT100:N2200 (2:1, wt:wt) and device D: NT00:NT100:N2200 (1.2:0.8:1, wt:wt:wt).

8. Grazing incidence wide-angle X-ray scattering (GIWAXS) Measurements
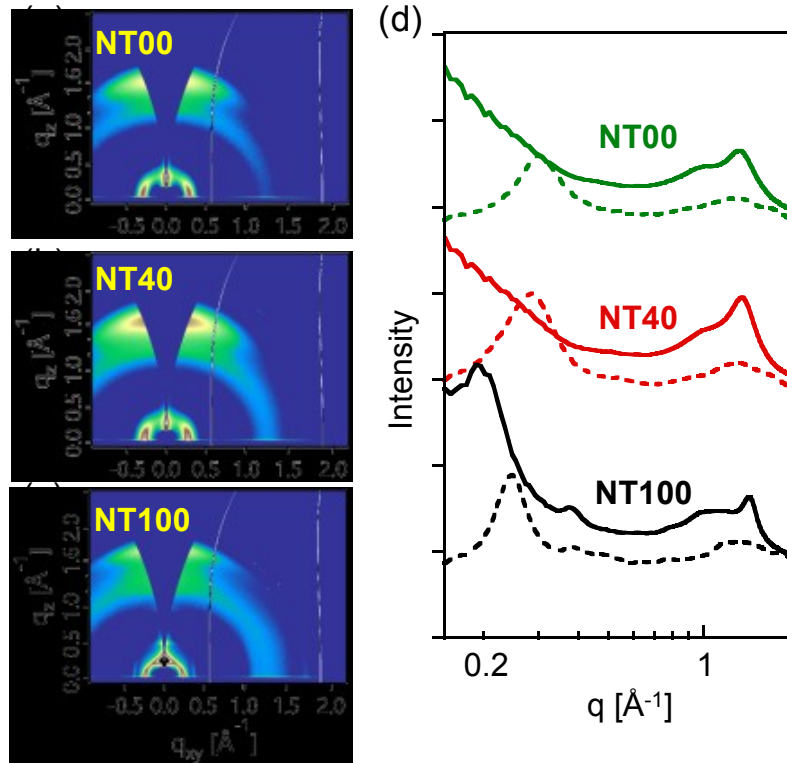
Fig. S8 GIWAXS (a-c) 2D patterns and (d) corresponding lint-cuts in OOP (solid lines) and IP (dashed lines) directions of neat NT00, NT40, and NT100 films.

9. Tapping-mode atomic force microscopy (AFM) Measurements
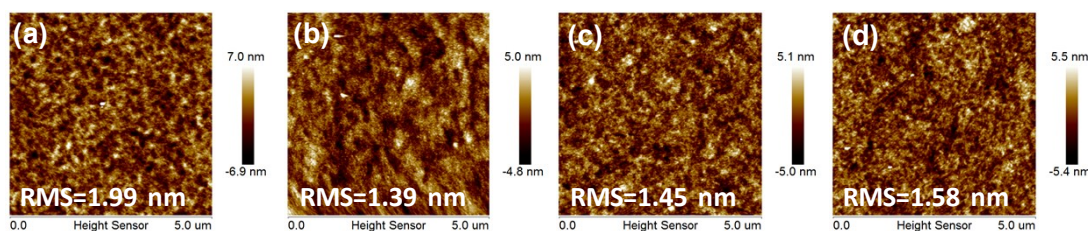
Fig. S9 AFM height images (5 μm × 5 μm) of NT00:N2200, NT40:N2200, NT100:N2200, and NT00:NT100:N2200 blend films.

10. References

(1) Jin, Y.; Chen, Z.; Dong, S.; Zheng, N.; Ying, L.; Jiang, X. F.; Liu, F.; Huang, F.; Cao, Y. A Novel Naphtho[1,2-*c*:5,6-*c*']Bis([1,2,5]Thiadiazole)-Based Narrow-Bandgap π-Conjugated Polymer with Power Conversion Efficiency Over 10%. *Adv. Mater.* **2016,** *28*, 9811-9818.

(2) Yan, H.; Chen, Z.; Zheng, Y.; Newman, C.; Quinn, J. R.; Dötz, F.; Kastler, M.; Facchetti, A. A High-Mobility Electron-Transporting Polymer for Printed Transistors. *Nature* **2009,** *457*, 679-686.